Electronic Supplementary Information

Syntheses, structural modulation and slow magnetic relaxation of three dysprosium(III) complexes with mononuclear, dinuclear and one-dimensional structures

Hua-Jian Ye,[a] Tian Zhang,[a] Shu-Yuan Huang,[a] Xiao-Ling Liu,[a] Wen-Bin Chen,*[a] Yi-Quan zhang,*[b] Jinkui Tang*[c] and Wen Dong*[a]

[a]Guangzhou Key Laboratory for Environmentally Functional Materials and Technology, School of Chemistry and Chemical Engineering, Guangzhou University, Guangzhou 510006, P. R. China

[b]Jiangsu Key Laboratory for NSLSCS, School of Physical Science and Technology, Nanjing Normal University, Nanjing 210023, P. R. China

[c]State Key Laboratory of Rare Earth Resource Utilization, Changchun Institute of Applied Chemistry, Chinese Academy of Sciences, Changchun 130022, P. R. China

Contents of the Electronic Supplementary Information

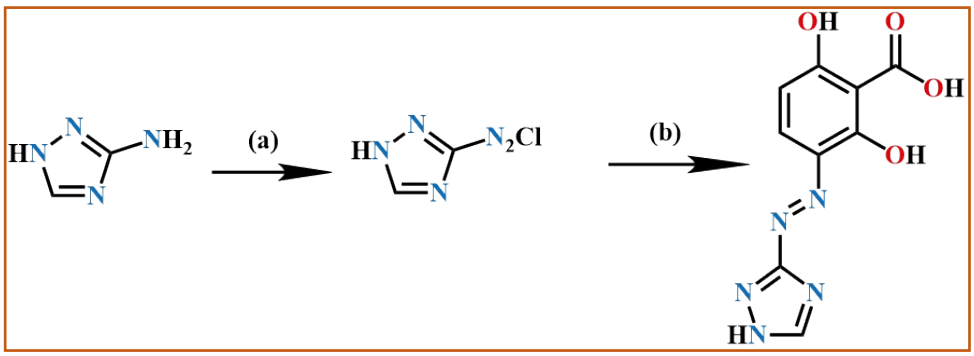

Scheme S1 Syntheses of H_4ATB: (a) HCl, 0–5 °C, $NaNO_2$, stirring; (b) 2,6-dihydroxybenzoic acid, stirring at room temperature.

Table S1. **1-3** geometry analysis by using SHAPE 2.0 program.*

	CSAPR-9 (C_{4v})	TCTPR-9 (D_{3h})	JCSAPR-9 (C_{4v})	JTCTPR-9 (D_{3h})	MFF-9 (C_S)
1	2.12956	2.30852	2.81009	**1.95785**	2.40949
2	**0.26965**	1.33393	0.83299	2.69822	0.88793
3	**0.31048**	1.30690	0.78641	2.40376	0.97232

*CSAPR-9=Spherical capped square antiprism;
TCTPR-9=Spherical tricapped trigonal prism;
JCSAPR-9=Capped square antiprism J10;
JTCTPR-9=Tricapped trigonal prism J51;
MFF-9=Muffin

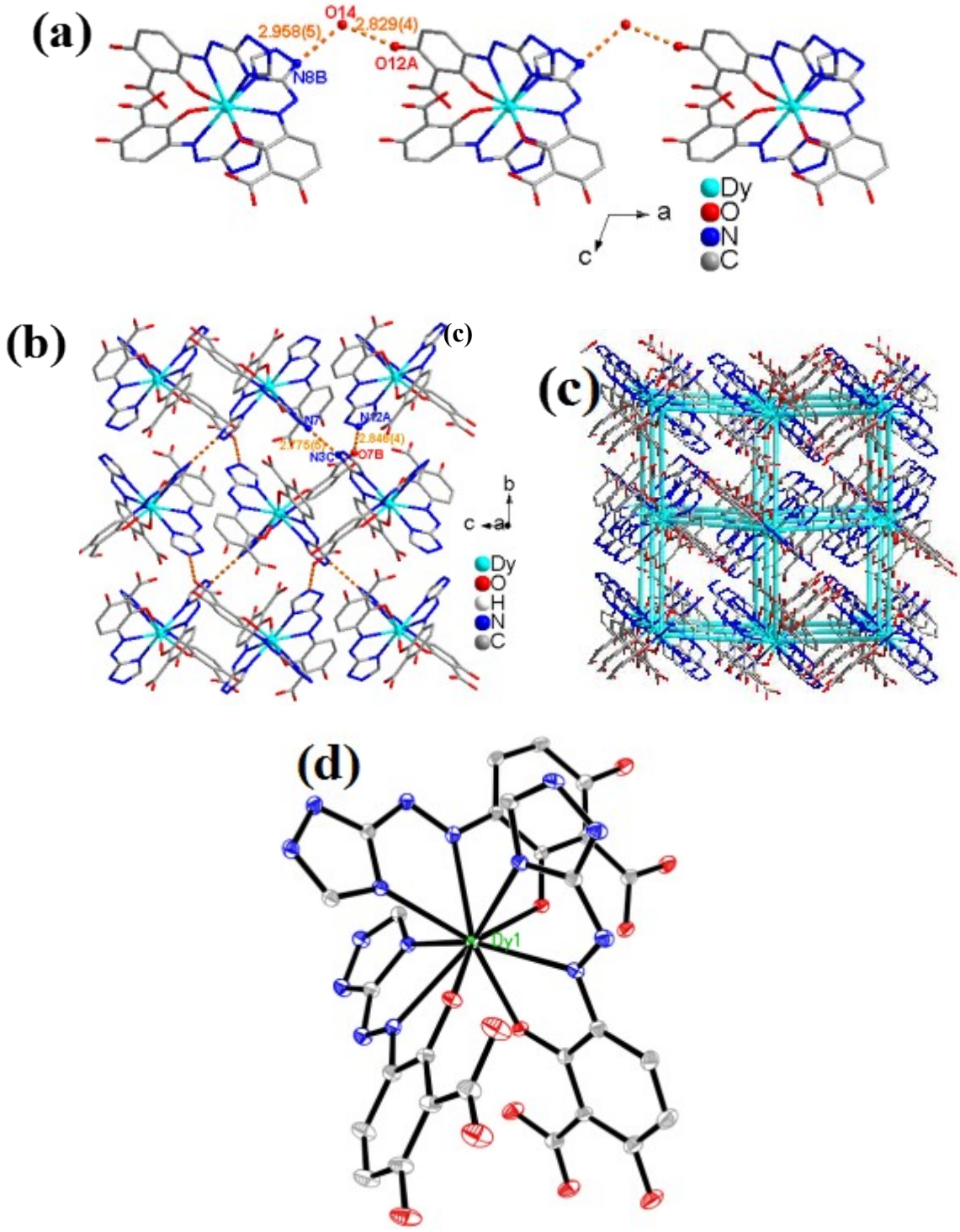

Fig. S1 For **1**, (a)hydrogen bonds along the *b* axis, (b) hydrogen bonds along the *b* axis and *c* axis, (c) 3D supramolecular structure (the blue lines between the dysprosium are just for observation, without any interaction), (d) ORTEP view (30% thermal ellipsoids).

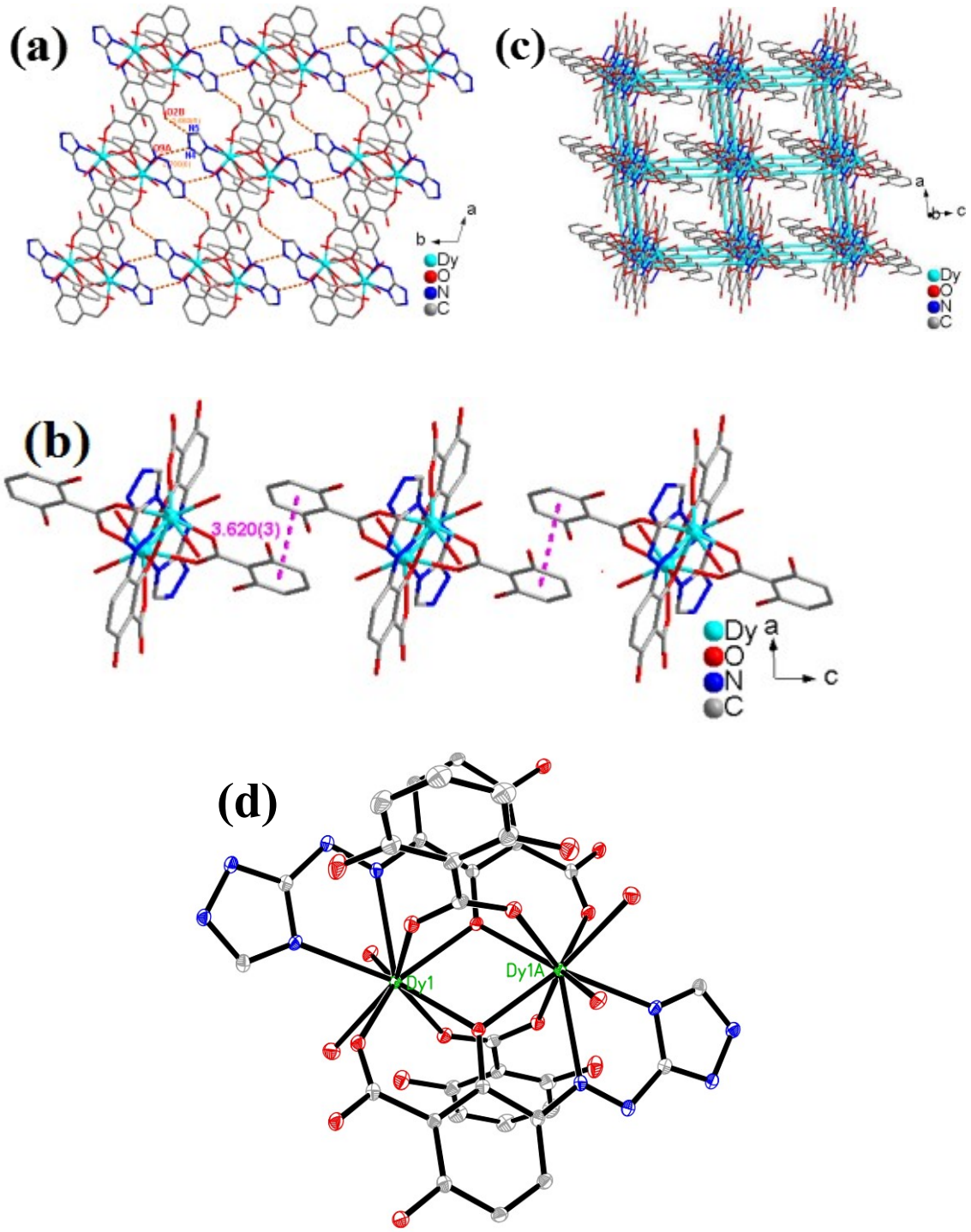

Fig. S2 For **2**, (a) hydrogen bonds along the *a* axis and *b* axis, (b) the π–π stacking interaction along the c-axis, (c) 3D supramolecular structure (the blue lines between the dysprosium are just for observation, without any interaction), (d) ORTEP view (30% thermal ellipsoids).

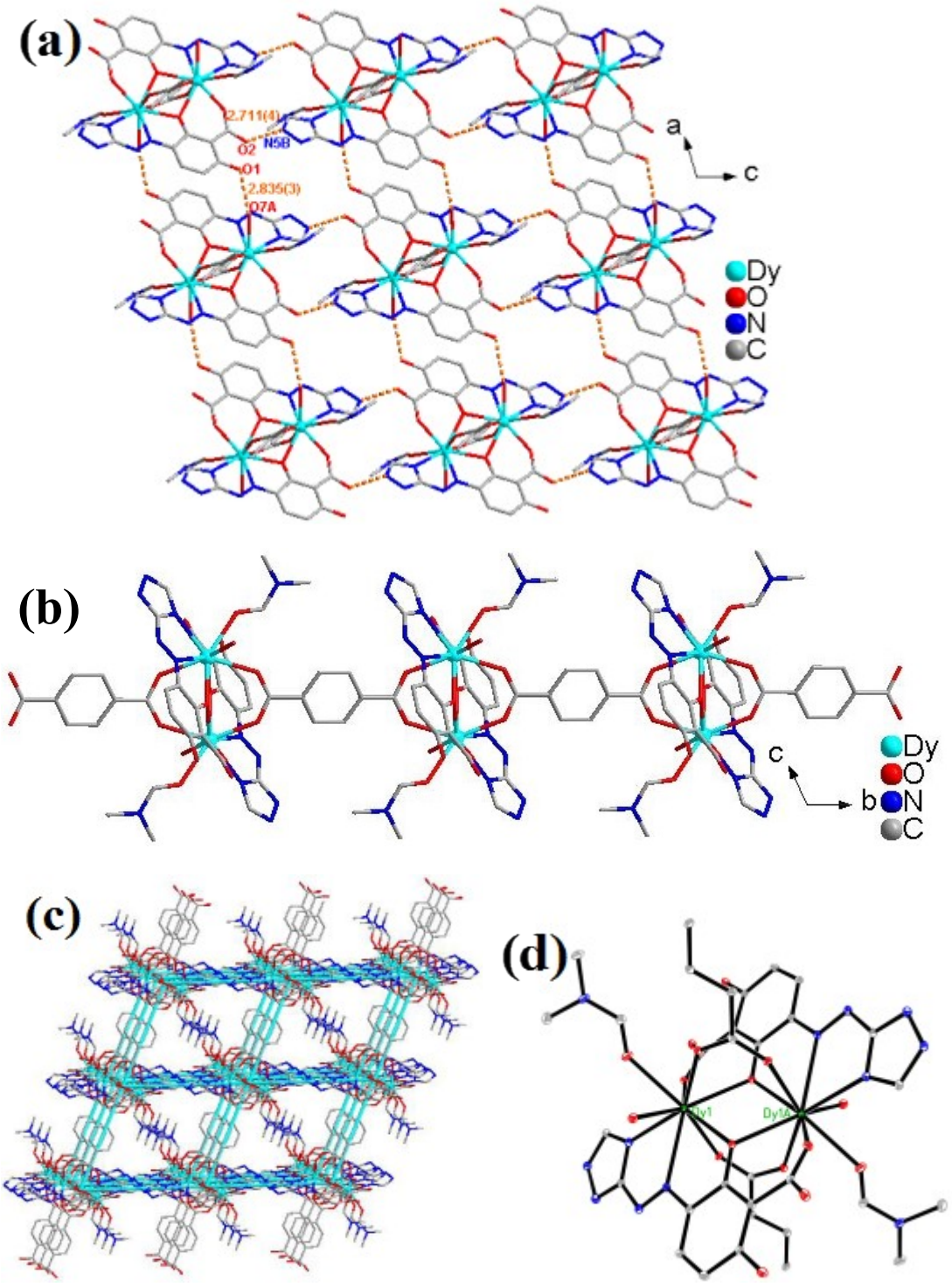

Fig. S3 For **3**, (a) hydrogen bonds along the *a* axis and *c* axis, (b) One-dimensional structure along the *b* axis, (c) 3D supramolecular structure (the blue lines between the dysprosium are just for observation, without any interaction), (d) ORTEP view (30% thermal ellipsoids).

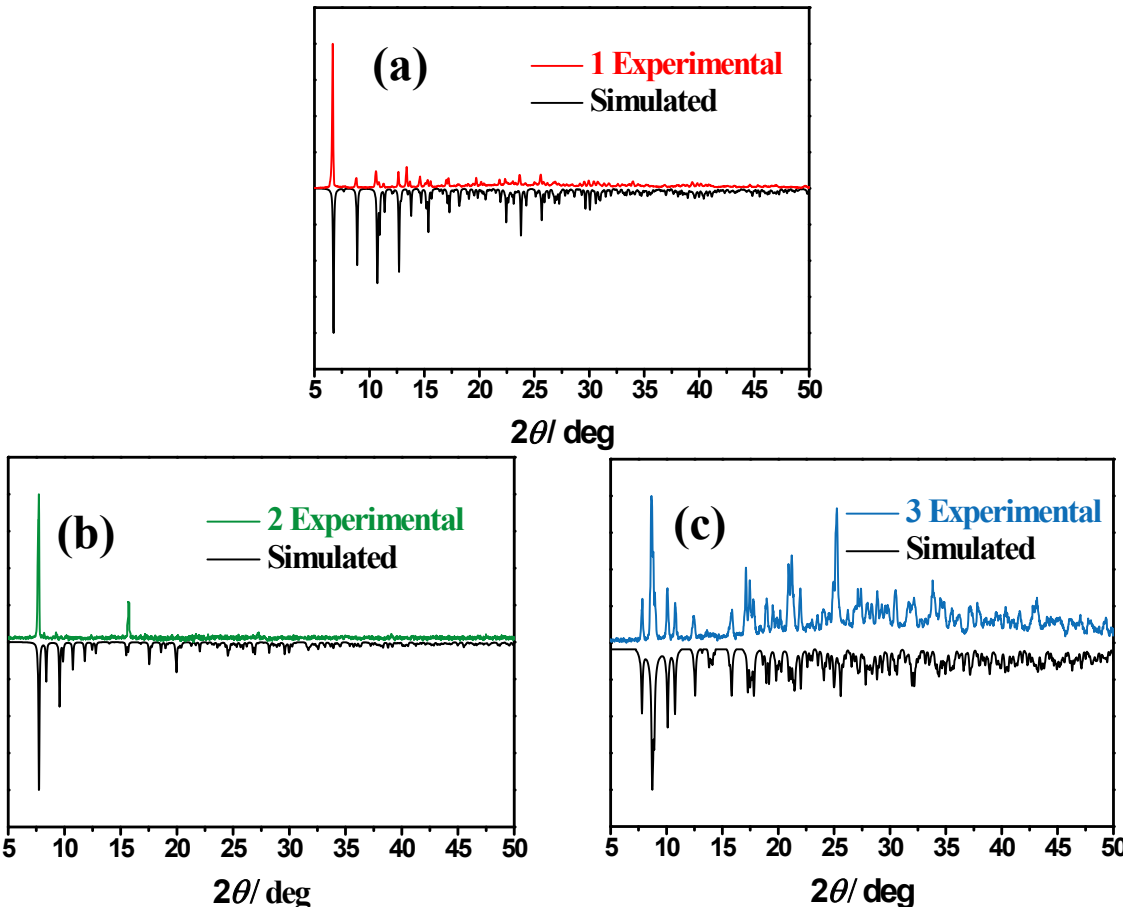

Fig. S4 Powder X-ray diffraction (PXRD) patterns for complexes **1-3**

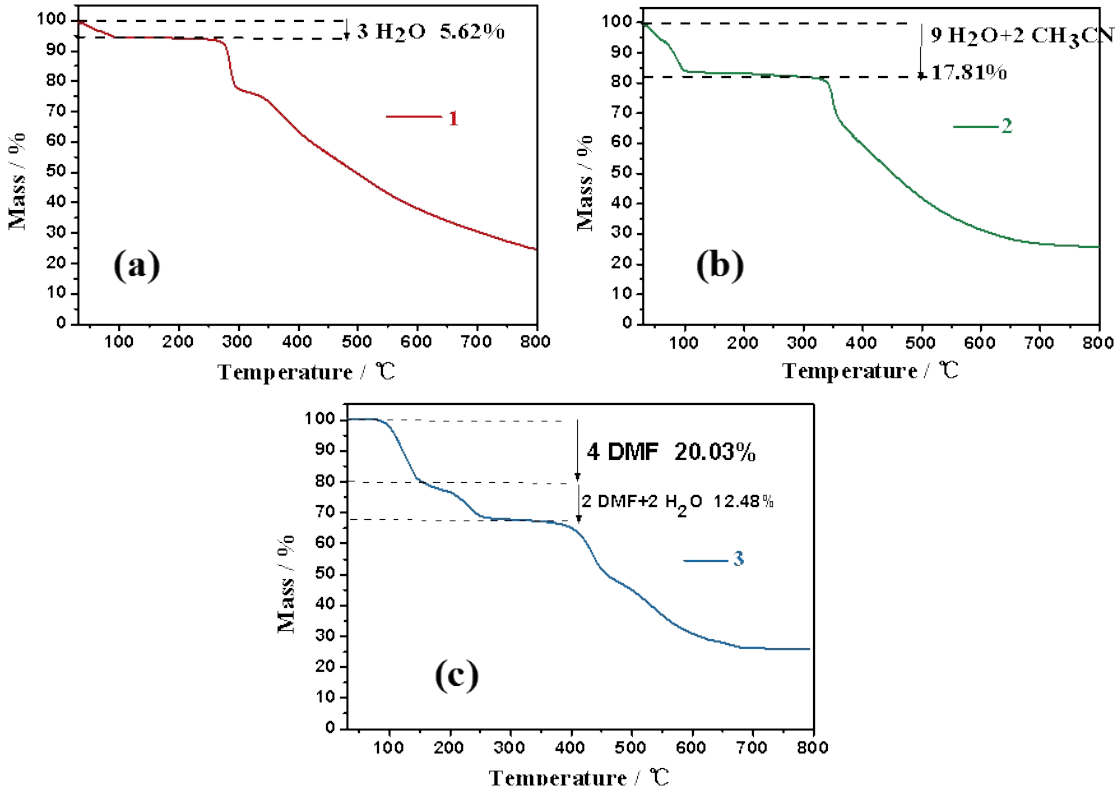

Fig. S5 TG curves of complexes **1-3.**

Table S2 Crystal data and structure refinement complexes **1-3**.

	1	**2**	**3**
Empirical formula	$C_{27}H_{24}DyN_{15}O_{15}$	$C_{36}H_{44}Dy_2N_{12}O_{25}$	$C_{22}H_{30}DyN_8O_{10}$
Formula weight	961.11	1369.83	729.04
Crystal system	monoclinic	triclinic	triclinic
Space group	$P2_1/c$	$P\bar{1}$	$P\bar{1}$
a/Å	13.96209(10)	9.6507(3)	10.56300(10)
b/Å	16.44139(8)	11.3380(2)	11.32340(10)
c/Å	17.20872(11)	11.8034(4)	12.71470(10)
α/°	90	103.705(2)	112.6490(10)
β/°	110.0249(7)	90.636(2)	100.3860(10)
γ/°	90	106.159(2)	98.7410(10)
Volume/Å^3	3711.54(4)	1201.07(6)	1338.83(2)
Z	4	1	2
ρ_{calc}g/cm^3	1.720	1.894	1.808
μ/mm^{-1}	11.564	17.346	15.554
F(000)	1908.0	676.0	728.0
Reflections collected	50442	14773	17175
Independent reflections	7632	4814	5387
R(int)	0.0355	0.0604	0.0413
Goodness-of-fit on F^2	1.100	1.077	1.101
Final R indexes [I>=2sigma (I)][a,b]	R_1 = 0.0308, wR_2 = 0.0787	R_1 = 0.0419, wR_2 = 0.1138	R_1 = 0.0288, wR_2 = 0.0769
R indexes [all data]	R_1 = 0.0322, wR_2 = 0.0795	R_1 = 0.0438, wR_2 = 0.1150	R_1 = 0.0295, wR_2 = 0.0774
Largest diff. peak/hole / e Å^{-3}	0.95/-1.04	2.65/-1.28	1.13/-1.26
CCDC	2098134	2098135	2098136

[a]$R_1 = \sum||F_o|-|F_c||/\sum|F_o|$. [b]$wR_2 = [\sum w(F_o^2 - F_c^2)^2/\sum w(F_o^2)^2]^{1/2}$

Table S3 The bond lengths [Å] and angles [°] for complex **1**.

Atom	Atom	[Å]		Atom	Atom	Atom	[°]
Dy1	O1	2.3375(19)		O1	Dy1	O9	85.51(7)
Dy1	O5	2.3049(19)		O1	Dy1	N1	125.25(7)
Dy1	O9	2.3413(19)		O1	Dy1	N5	64.82(7)
Dy1	N1	2.484(2)		O1	Dy1	N6	150.76(7)
Dy1	N5	2.586(2)		O1	Dy1	N10	138.50(7)
Dy1	N6	2.436(2)		O1	Dy1	N11	89.77(7)
Dy1	N10	2.589(2)		O1	Dy1	N15	70.99(7)
Dy1	N11	2.507(2)		O5	Dy1	O1	77.84(7)
Dy1	N15	2.585(3)		O5	Dy1	O9	147.69(7)
Atom	**Atom**	**Atom**	**[°]**	O5	Dy1	N1	83.29(7)
N1	Dy1	N11	138.79(8)	O5	Dy1	N5	79.59(7)
N1	Dy1	N15	144.21(8)	O5	Dy1	N6	126.67(7)
N5	Dy1	N10	121.25(7)	O5	Dy1	N10	64.70(7)
N5	Dy1	N15	77.88(8)	O5	Dy1	N11	84.15(7)
N6	Dy1	N1	129.10(8)	O5	Dy1	N15	132.44(7)
N6	Dy1	N5	61.98(7)	O9	Dy1	N1	84.09(7)
N6	Dy1	N10	78.70(8)	O9	Dy1	N5	68.25(7)
N6	Dy1	N11	79.94(8)	O9	Dy1	N6	79.01(7)
N6	Dy1	N15	152.13(8)	O9	Dy1	N10	135.94(7)
N11	Dy1	N5	70.02(7)	O9	Dy1	N11	123.66(7)
N11	Dy1	N10	61.24(8)	O9	Dy1	N15	64.26(7)
N11	Dy1	N15	115.97(8)	N1	Dy1	N5	61.39(8)
N15	Dy1	N10	122.65(8)	N1	Dy1	N10	69.11(7)

Table S4 The bond lengths [Å] and angles [°] for complex **2**.

Atom	Atom	[Å]	Atom	Atom	Atom	[°]
Dy1	Dy1[1]	3.7652(4)	O3	Dy1	Dy1[1]	107.29(7)
Dy1	O3	2.300(3)	O3	Dy1	O4[1]	141.57(10)
Dy1	O4[1]	2.384(3)	O3	Dy1	O4	72.04(10)
Dy1	O4	2.367(3)	O3	Dy1	O6[1]	110.94(10)
Dy1	O6[1]	2.396(3)	O3	Dy1	O7	75.17(11)
Dy1	O7	2.394(3)	O3	Dy1	O9	138.16(10)
Dy1	O9	2.446(3)	O3	Dy1	O10	71.61(11)
Dy1	O10	2.435(3)	O3	Dy1	N1[1]	125.68(11)
Dy1	N1[1]	2.602(4)	O3	Dy1	N3[1]	73.47(11)
Dy1	N3[1]	2.484(3)	O4[1]	Dy1	Dy1[1]	37.73(7)
Atom	**Atom**	**Atom** **[°]**	O4	Dy1	Dy1[1]	37.42(7)
O6[1]	Dy1	N1[1] 123.12(11)	O4[1]	Dy1	O4	75.15(11)
O6[1]	Dy1	N3[1] 142.03(11)	O4	Dy1	O6[1]	76.15(10)
O7	Dy1	Dy1[1] 72.88(7)	O4[1]	Dy1	O6[1]	76.15(10)
O7	Dy1	O9 132.68(10)	O4[1]	Dy1	O7	77.67(10)
O7	Dy1	O10 141.71(11)	O4	Dy1	O7	75.34(10)
O7	Dy1	N1[1] 66.21(11)	O4[1]	Dy1	O9	75.34(10)
O7	Dy1	N3[1] 75.98(11)	O4	Dy1	O9	110.93(10)
O9	Dy1	Dy1[1] 110.72(7)	O4[1]	Dy1	O10	140.54(10)
O9	Dy1	N1[1] 66.52(10)	O4	Dy1	O10	128.01(10)
O9	Dy1	N3[1] 83.60(11)	O4	Dy1	N1[1]	63.77(10)
O10	Dy1	Dy1[1] 135.36(8)	O4[1]	Dy1	N1[1]	63.77(10)
O10	Dy1	O9 69.30(10)	O4	Dy1	N3[1]	139.56(11)
O10	Dy1	N1[1] 120.99(11)	O4[1]	Dy1	N3[1]	124.91(11)
O10	Dy1	N3[1] 76.78(11)	O6[1]	Dy1	Dy1[1]	69.50(7)
N1[1]	Dy1	Dy1[1] 96.43(7)	O6[1]	Dy1	O7	141.97(10)
N3[1]	Dy1	Dy1[1] 147.31(8)	O6[1]	Dy1	O9	68.32(10)
N3[1]	Dy1	N1[1] 61.44(11)	O6[1]	Dy1	O10	69.79(11)

[1]1-X,1-Y,1-Z

Table S5 The bond lengths [Å] and angles [°] for complex **3**.

Atom	Atom	[Å]or[°]	Atom	Atom	Atom	[Å]or[°]
Dy1	Dy1[1]	3.7943(3)	O3[1]	Dy1	Dy1[1]	37.63(5)
Dy1	O3[1]	2.3938(18)	O3	Dy1	Dy1[1]	37.59(4)
Dy1	O3	2.3959(19)	O3[1]	Dy1	O3	75.22(7)
Dy1	O4	2.3480(19)	O3	Dy1	O6	113.31(7)
Dy1	O5[1]	2.3816(18)	O3[1]	Dy1	O6	144.39(7)
Dy1	O6	2.464(2)	O3[1]	Dy1	O7	80.92(7)
Dy1	O1	2.344(2)	O3	Dy1	O7	140.23(7)
Dy1	O7	2.406(2)	O3	Dy1	N1[1]	126.64(7)
Dy1	N1[1]	2.596(2)	O3[1]	Dy1	N1[1]	63.99(7)
Dy1	N3[1]	2.513(2)	O3	Dy1	N3[1]	136.92(7)
Atom	**Atom**	**Atom** **[Å]or[°]**	O3[1]	Dy1	N3[1]	124.80(7)
O6	Dy1	N3[1] 73.92(7)	O4	Dy1	Dy1[1]	70.26(5)
O1	Dy1	Dy1[1] 106.19(5)	O4	Dy1	O3	73.41(7)
O1	Dy1	O3 70.96(6)	O4	Dy1	O3[1]	75.55(6)
O1	Dy1	O3[1] 140.22(7)	O4	Dy1	O5[1]	140.56(6)
O1	Dy1	O4 75.23(7)	O4	Dy1	O6	139.80(7)
O1	Dy1	O5[1] 108.93(7)	O4	Dy1	O7	130.24(7)
O1	Dy1	O6 70.65(7)	O4	Dy1	N1[1]	64.48(7)
O1	Dy1	O7 138.86(7)	O4	Dy1	N3[1]	76.03(7)
O1	Dy1	N1[1] 123.66(7)	O5[1]	Dy1	Dy1[1]	71.05(5)
O1	Dy1	N3[1] 72.39(7)	O5[1]	Dy1	O3	71.47(7)
O7	Dy1	Dy1[1] 112.69(5)	O5[1]	Dy1	O3[1]	78.66(6)
O7	Dy1	O6 71.19(7)	O5[1]	Dy1	O6	72.40(7)
O7	Dy1	N1[1] 65.83(7)	O5[1]	Dy1	O7	72.97(7)
O7	Dy1	N3[1] 82.85(7)	O5[1]	Dy1	N1[1]	127.30(7)
N1[1]	Dy1	Dy1[1] 95.75(5)	O5[1]	Dy1	N3[1]	143.33(7)
N3[1]	Dy1	Dy1[1] 145.20(5)	O6	Dy1	Dy1[1]	139.71(5)
N3[1]	Dy1	N1[1] 61.18(7)	O6	Dy1	N1[1]	119.95(7)

[1]1-X,1-Y,1-Z; [2]1-X,-Y,1-Z

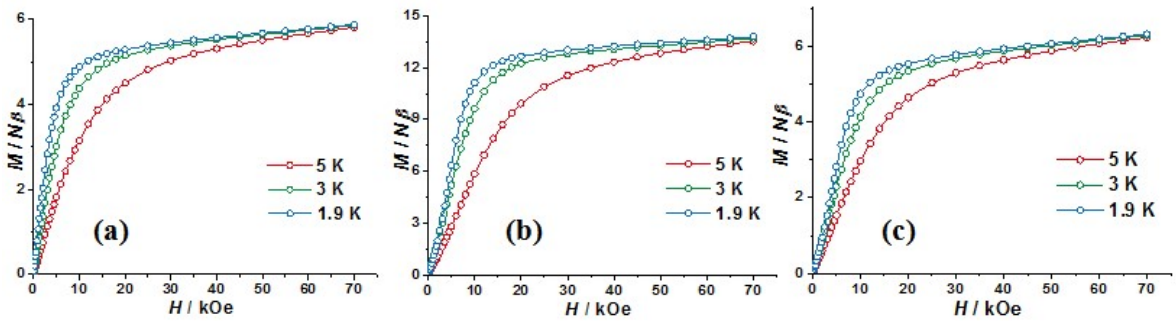

Fig. S6 The isothermal M vs. H plots for **1-3** (a-c), respectively.

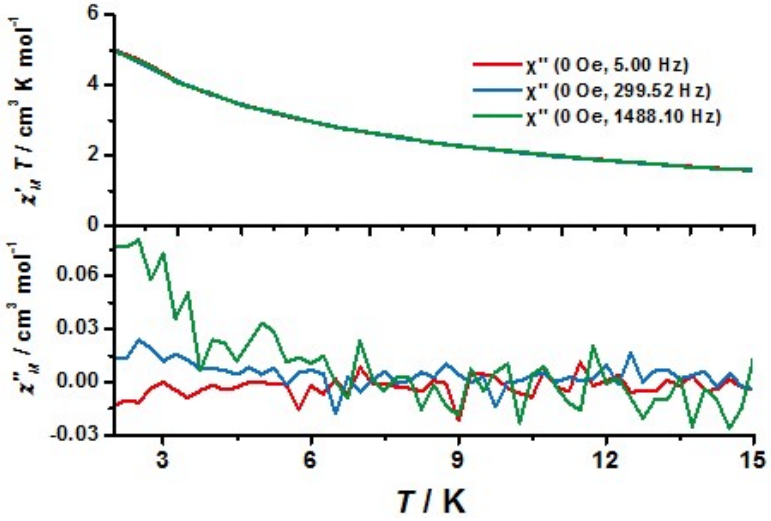

Fig. S7 Temperature dependence of the in-phase χM' product and out-of-phase χ_M'' for **1** in a zero dc field with an ac frequency of 3.0 Oe.

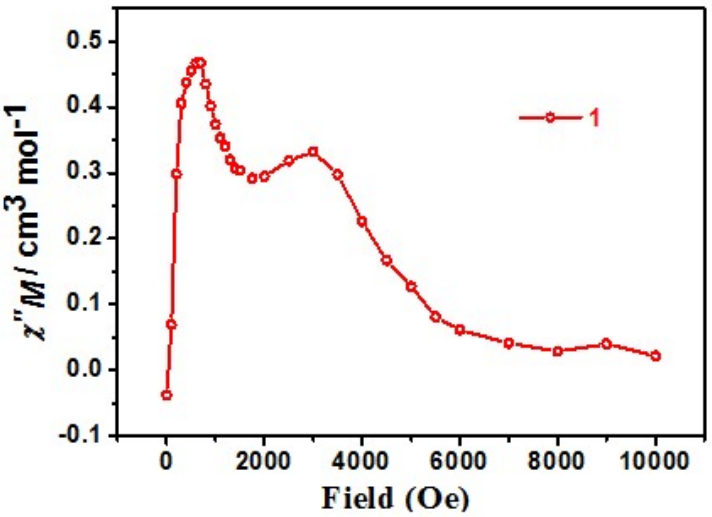

Fig. S8 Ac susceptibilities of **1** were measured at 1.9 K under different fields to find an optimum dc field for suppressing the QTM.

Table S6 Relaxation fitting parameters from Least-Squares Fitting of χ(ω) data for **1** at 600 Oe dc field.

T / K	τ	τ	α	α	χ_0	χ_0	χ_∞	χ_∞
	Value	Standard Error	Value	Standard Error	Value	Standard Error	Value	Standard Error
2	0.00336	7.30368E-5	0.27104	0.00923	5.30749	0.02575	1.02005	0.02869
2.5	0.0013	2.23455E-5	0.21796	0.00773	4.42126	0.01341	0.8828	0.02434
3	5.54124E-4	9.96266E-6	0.19264	0.00766	3.79593	0.0088	0.7912	0.02611
3.5	2.66291E-4	3.94232E-6	0.16664	0.00554	3.30826	0.00414	0.76952	0.02076
4	1.27819E-4	1.58288E-6	0.16514	0.00331	2.93126	0.00154	0.69645	0.01592
4.5	5.28665E-5	2.24833E-6	0.21147	0.00608	2.63475	0.00164	0.49396	0.05009
5	0.00336	3.35116E-6	0.26868	0.00938	2.39407	0.00124	0.51274	0.14594

Table S7 Relaxation fitting parameters from Least-Squares Fitting of χ(ω) data for **2** at 0 Oe dc field.

T / K	τ	τ	α	α	χ_0	χ_0	χ_∞	χ_∞
	Value	Standard Error	Value	Standard Error	Value	Standard Error	Value	Standard Error
9	4.89537E-5	2.84144E-6	0.11883	0.00927	2.96581	0.00112	1.85205	0.04212
8	1.38889E-4	4.99503E-6	0.16349	0.01011	3.24829	0.00321	1.78567	0.03027
7	2.481E-4	1.83229E-5	0.28244	0.01914	3.59171	0.01262	1.35758	0.07417
6	3.01702E-4	2.04796E-5	0.36673	0.01451	4.00342	0.01884	0.20649	0.09857
5.5	5.71723E-4	1.39014E-5	0.31729	0.00745	4.20031	0.01234	0.14471	0.03963
5	0.00114	1.3009E-5	0.27391	0.00448	4.4083	0.00929	0.16692	0.01875
4.5	0.00223	2.10839E-5	0.25373	0.0041	4.64605	0.01049	0.20611	0.01448
4	0.00398	4.93017E-5	0.25969	0.00537	4.9078	0.01688	0.23615	0.0172
3.5	0.00601	8.78741E-5	0.28817	0.00599	5.17077	0.02294	0.21666	0.01877
3	0.00765	1.0765E-4	0.30809	0.00548	5.34603	0.02388	0.2024	0.01704
2.5	0.00885	1.24442E-4	0.31718	0.00532	5.35255	0.02448	0.19667	0.01606
2	0.01006	1.46495E-4	0.32653	0.00533	5.05001	0.02431	0.19316	0.01478

Table S8 Relaxation fitting parameters from Least-Squares Fitting of χ(ω) data for **3** at 0 Oe dc field.

T / K	τ	τ	α	α	χ_0	χ_0	χ_∞	χ_∞
	Value	Standard Error	Value	Standard Error	Value	Standard Error	Value	Standard Error
2	3.65489E-4	9.3868E-6	0.20189	0.00966	2.60338	0.00663	0.54128	0.02669
2.3	3.37087E-4	8.8007E-6	0.19943	0.00965	2.6456	0.00645	0.575	0.02758
2.6	2.79968E-4	8.13193E-6	0.20345	0.00997	2.63286	0.00611	0.59754	0.03044
2.9	2.14292E-4	6.32298E-6	0.20433	0.00909	2.58403	0.00475	0.64451	0.02994
3.2	1.57409E-4	6.13492E-6	0.21512	0.01012	2.51841	0.00431	0.70017	0.03682
3.5	1.29624E-4	6.20224E-6	0.22258	0.01105	2.44343	0.00384	0.81732	0.04015
4	1.19673E-4	4.34051E-6	0.21043	0.0091	2.31485	0.00306	1.05256	0.02458
4.5	9.45254E-5	2.7406E-6	0.18555	0.0067	2.17963	0.00153	1.1791	0.01634
5	3.80414E-5	3.71468E-6	0.21272	0.01138	2.0564	0.00116	1.04542	0.05554
6	2.46888E-5	8.70605E-6	0.21779	0.0261	1.83649	5.64746E-4	1.55209	0.05959

Computational details

Mononuclear complex **1** has one type of molecular structure, and binuclear complexes **2** and **3** with central symmetrical structure also have only one type of magnetic center Dy^{III} ion indicated as **2_Dy1** and **3_Dy1**. Complete-active-space self-consistent field (CASSCF) calculations on complex **1** and individual Dy^{III} fragments of **2** and **3** (see Figure S9 for the calculated complete structures of **1**–**3**) on the basis of single-crystal X-ray determined geometries have been carried out with MOLCAS 8.4[S1] program package. Each individual Dy^{III} fragment in **2** and **3** was calculated keeping the experimentally determined structure of the corresponding compound while replacing the neighboring Dy^{III} ion by diamagnetic Lu^{III}.

The basis sets for all atoms are atomic natural orbitals from the MOLCAS ANO-RCC library: ANO-RCC-VTZP for Dy^{III}; VTZ for close N and O; VDZ for distant atoms. The calculations employed the second order Douglas-Kroll-Hess Hamiltonian, where scalar relativistic contractions were taken into account in the basis set and the spin-orbit couplings were handled separately in the restricted active space state interaction (RASSI-SO) procedure.[S2–S3] For individual Dy^{III} fragment, active electrons in 7 active orbitals include all f electrons (CAS (9 in 7)) in the CASSCF calculation. To exclude all the doubts, we calculated all the roots in the active space. We have mixed the maximum number of spin-free state which was possible with our hardware (all from 21

sextets, 128 from 224 quadruplets, 130 from 490 doublets). SINGLE_ANISO[S4-S6] program was used to obtain the energy levels, $\boldsymbol{g}$ tensors, m_J values, magnetic axes, *et al.* based on the above CASSCF/RASSI-SO calculations.

To fit the exchange interactions between Dy^{III} ions in complexes **2** and **3**, we took two steps to obtain them. Firstly, we calculated individual Dy^{III} fragments using CASSCF/RASSI-SO to obtain the corresponding magnetic properties. Then, the exchange interaction between the magnetic centers was considered within the Lines model,[S7] while the account of the dipole-dipole magnetic coupling is treated exactly. The Lines model is effective and has been successfully used widely in the research field of d and f-elements single-molecule magnets.[S8–S9]

The Ising exchange Hamiltonian for **2** and **3** is: $\boldsymbol{H}_{exch} = -\boldsymbol{J}\boldsymbol{S}_{Dy1}\boldsymbol{S}_{Dy2}$

The $\boldsymbol{J} = 25 \cos\varphi J$, where φ is the angle between the anisotropy axes on two Dy^{III} sites, and J is the Lines exchange coupling parameter. $\boldsymbol{S}_{Dy} = 1/2$ is the ground pseudospin on the Dy^{III} site. $\boldsymbol{J}_{total}$ is the parameter of the total magnetic interaction ($\boldsymbol{J}_{total}=\boldsymbol{J}_{dip}+\boldsymbol{J}_{exch}$) between magnetic center ions. The dipolar magnetic coupling can be calculated exactly, while the exchange coupling constants were fitted through comparison of the computed and measured magnetic susceptibilities using POLY_ANISO program.[S4–S6]

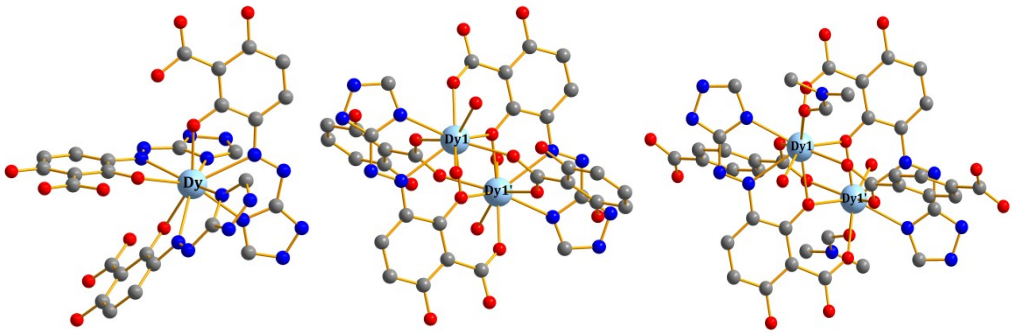

Figure S9. Calculated complete structures of **1**–**3**; H atoms are omitted for clarify.

Table S9. Calculated energy levels (cm^{-1}), $\boldsymbol{g}$ (g_x, g_y, g_z) tensors and predominant m_J values of the lowest eight Kramers doublets (KDs) of complex **1** and individual Dy^{III} fragments for complexes **2** and **3** using CASSCF/RASSI-SO with MOLCAS 8.4.

KDs	**1**			**2_Dy1**			**3_Dy1**		
	E/cm^{-1}	$\boldsymbol{g}$	m_J	E/cm^{-1}	$\boldsymbol{g}$	m_J	E/cm^{-1}	$\boldsymbol{g}$	m_J
1	0.0	0.003 0.003 19.740	±15/2	0.0	0.030 0.068 19.525	±15/2	0.0	0.079 0.206 19.118	±15/2
2	110.1	0.905 1.957 13.450	±13/2	48.8	0.177 0.225 16.714	±13/2	29.3	1.848 2.823 15.955	±11/2
3	153.4	0.730 3.180 12.073	±5/2	133.5	1.625 2.229 11.765	±11/2	54.7	3.703 5.098 9.118	±13/2
4	245.6	0.065 4.764 9.729	±11/2	171.5	2.113 4.747 11.167	±5/2	90.4	0.895 4.104 10.091	±9/2
5	299.2	4.005 4.819 11.503	±9/2	213.1	3.109 4.711 11.389	±7/2	147.6	1.248 2.141 13.250	±7/2
6	372.8	0.196 1.485 16.669	±7/2	296.4	0.719 2.492 15.309	±3/2	214.0	0.371 0.627 16.808	±5/2
7	413.4	1.223 2.092 15.275	±3/2	335.4	1.148 1.643 17.625	±1/2	324.0	0.075 0.127 16.606	±3/2
8	506.3	0.316 0.435 17.922	±1/2	399.0	0.125 0.362 19.038	±9/2	364.2	0.053 0.202 17.862	±1/2

Table S10. Wave functions with definite projection of the total moment | m_J > for the lowest eight KDs of complex **1** and individual Dy^{III} fragments for complexes **2** and **3** using CASSCF/RASSI-SO with MOLCAS 8.4.

	E/cm^{-1}	wave functions
1	0.0	95.00 %|±15/2>
	110.1	65.60%|±13/2>+8.5%|±1/2>+7.3%|±3/2>+5.9%|±11/2>+5.9%|±7/2>
	153.4	33.1%|±1/2>+23.1%|±3/2>+13.2%|±5/2>+12.6%|±13/2>+9.9%|±11/2>
	245.6	28.6%|±11/2>+18.7%|±9/2>+14.1%|±13/2>+12.6%|±3/2>+11.6%|±7/2>
	299.2	33.5%|±11/2>+22.7%|±5/2>+19.2%|±7/2>+13.9%|±9/2>+4.0%|±3/2>
	372.8	30.0%|±9/2>+24.6%|±7/2>+12.7%|±11/2>+12.3%|±3/2>+9.9%|±5/2>
	413.4	28.7%|±1/2>+20.1%|±9/2>+18.7%|±3/2>+13.6%|±7/2>+13.2%|±5/2>
	506.3	27.0%|±5/2>+22.1%|±7/2>+21.8%|±3/2>+15.1%|±1/2>+9.7%|±9/2>
2_Dy1	0.0	96.2%|±15/2>
	48.8	93.4%|±13/2>
	133.5	71.2%|±11/2>+10.1%|±3/2>+8.3%|±1/2>+4.5%|±9/2>
	171.5	26.3%|±9/2>+22.9%|±1/2>+18.7%|±3/2>+12.3%|±5/2>+11.9%|±7/2>
	213.1	29.4%|±7/2>+28.3%|±5/2>+19.3%|±3/2>+6.9%|±1/2>+6.8%|±9/2>
	296.4	22.0%|±1/2>+21.5%|±5/2>+19.3%|±3/2>+19.0%|±9/2>+14.6%|±7/2>
	335.4	37.1%|±1/2>+33.9%|±3/2>+12.3%|±7/2>+10.9%|±5/2>
	399.0	30.3%|±5/2>+30.1%|±7/2>+15.9%|±9/2>+10.7%|±3/2>+7.5%|±11/2>
3_Dy1	0.0	91.0%|±15/2>
	29.3	25.4%|±9/2>+19.8%|±13/2>+15.6%|±7/2>+14.3%|±11/2>+11.3%|±5/2>+7%|±5/2>
	54.7	50.8%|±13/2>+21.0%|±11/2>+14.9%|±7/2>+3.9%|±9/2>
	90.4	34.4%|±11/2>+20.6%|±13/2>+20.3%|±9/2>+11.3%|±5/2>+6.9%|±3/2>
	147.6	33.7%|±9/2>+22.2%|±7/2>+19.5%|±11/2>+7.0%|±1/2>+6.4%|±3/2>
	214.0	32.8%|±7/2>+31.1%|±5/2>+12.0%|±3/2>+11.2%|±9/2>+8.3%|±1/2>
	324.0	38.7%|±3/2>+35.2%|±5/2>+12.2%|±1/2>+10.7%|±7/2>
	364.2	61.4%|±1/2>+26.4%|±3/2>+4.1%|±5/2>

Table S11. Exchange energies E (cm^{-1}), the energy difference between each exchange doublets Δ_t (cm^{-1}) and the main values of the g_z for the lowest two exchange doublets of **2** and **3**.

	2			**3**		
	E	Δ_t	g_z	E	Δ_t	g_z
1	0.000000000000	1.955×10^{-5}	0.000	0.000000000000	2.204×10^{-4}	0.000
	0.000019550866			0.000220394298		
2	2.753181132228	3.437×10^{-5}	39.051	1.987569597334	3.338×10^{-4}	38.196
	2.753215506500			1.987903364877		

References:

S1 Aquilante, F.; Autschbach, J.; Carlson, R. K.; Chibotaru, L. F.; Delcey, M. G.; De Vico, L.; Galván, I. F.; Ferré, N.; Frutos, L. M.; Gagliardi, L.; Garavelli, M.; Giussani, A.; Hoyer, C. E.; Li Manni, G.; Lischka, H.; Ma, D.; Malmqvist, P. Å.; Müller, T.; Nenov, A.; Olivucci, M.; Pedersen, T. B.; Peng, D.; Plasser, F.; Pritchard, B.; Reiher, M.; Rivalta, I.; Schapiro, I.; Segarra-Martí, J.; Stenrup, M.; Truhlar, D. G.; Ungur, L.; Valentini, A.; Vancoillie, S.; Veryazov, V.; Vysotskiy, V. P.; Weingart, O.; Zapata, F.; Lindh, R. *J. Comput. Chem.* **2016**, *37*, 506−541.

S2 Malmqvist, P. Å.; Roos, B. O.; Schimmelpfennig, B. *Chem. Phys. Lett.,* **2002**, 357*,* 230–240.

S3 Heß, B. A.; Marian, C. M.; Wahlgren, U.; Gropen, O. *Chem. Phys. Lett.,* **1996**, 251*,* 365–371.

S4 Chibotaru, L. F.; Ungur, L.; Soncini, A. *Angew. Chem., Int. Ed*. **2008**, *47*, 4126–4129.

S5 Ungur, L.; Van den Heuvel, W.; Chibotaru, L. F. *New J. Chem.* **2009**, *33*, 1224–1230.

S6 Chibotaru, L. F.; Ungur, L.; Aronica, C.; Elmoll, H.; Pilet, G.; Luneau, D. *J. Am. Chem. Soc*. **2008**, *130*, 12445–12455.

S7 Lines, M. E. *J. Chem. Phys*. **1971**, *55*, 2977−2984.

S8 Mondal, K. C.; Sundt, A.; Lan, Y. H.; Kostakis, G. E.; Waldmann, O.; Ungur, L.; Chibotaru, L. F.; Anson, C. E.; Powell, A. K. *Angew. Chem., Int. Ed.* **2012**, *51*, 7550−7554.

S9 Langley, S. K.; Wielechowski, D. P.; Vieru, V.; Chilton, N. F.; Moubaraki, B.; Abrahams, B. F.; Chibotaru, L. F.; Murray, K. S. *Angew. Chem., Int. Ed.* **2013**, *52*, 12014–12019.